# Mineralizing fluid composition and genesis of gold–sulfide–telluride mineralization at the Megradzor deposit: Evidence from fluid inclusions

**Article** *in* Geochemistry International · January 2001

CITATION
1

READS
39

**6 authors**, including:

V. A. Kovalenker
Russian Academy of Sciences
**122** PUBLICATIONS **866** CITATIONS
SEE PROFILE

Vsevolod Yuriyevich Prokof'ev
Russian Academy of Sciences
**354** PUBLICATIONS **1,574** CITATIONS
SEE PROFILE

*Geochemistry International, Vol. 39, Suppl. 2, 2001, pp. S145–S159.*


# Mineralizing Fluid Composition and Genesis of Gold–Sulfide–Telluride Mineralization at the Megradzor Deposit: Evidence from Fluid Inclusions

**V. A. Kovalenker*, V. Yu. Prokof'yev*, S. V. Kozerenko**, O. F. Mironova**, N. N. Kolpakova**, and M. A. Zalibekyan*****

** Institute of the Geology of Ore Deposits, Petrography, Mineralogy, and Geochemistry, Russian Academy of Sciences, Staromonetnyi per. 35, Moscow, 109017 Russia*

*** Vernadsky Institute of Geochemistry and Analytical Chemistry, Russian Academy of Sciences, ul. Kosygina 19, Moscow, 117975 Russia*

**** Megradzor Mine, Megradzor, Armenia*

Received January 3, 2000

**Abstract**—Evidence provided by fluid inclusions points to a broad interval of physical conditions and fluid compositions at which the mineralization was produced: temperatures of 360–132°C, pressures of 2180–130 bar, fluid salinities of 18.5–1.4 wt % equiv. NaCl, 5.7–0.9 mol $CO_2$/kg of solution, and $4 \times 10^{-2}$ to $10^{-2}$ mol $H_2S$/kg of solution. The solutions are determined to contain Cl (0.77–0.24 mol/kg of solution), Na (0.7–0.3 mol/kg of solution), and K (0.14–$1.5 \times 10^{-3}$ mol/kg of solution). Thermodynamic calculations indicate that the most probable deposition factors of metals early in the mineralizing process were an increase in the pH and a decrease in the temperature, perhaps, due to the ascent of the mineralizing solution and its mixing with meteoric waters. The origin of the telluride mineralization was controlled by the involvement of fluids of other geneses (probably related to connate solutions) into the hydrothermal system. The early hydrothermal mineral assemblages are demonstrated to have been formed at relatively high temperatures and pressures by fluids compositionally most close to magmatic fluids. Gold-bearing mineral assemblages were deposited in environments most close to epithermal systems. The fact that gold-bearing mineral assemblages inherit certain features from early assemblages suggests that the Megradzor deposit was produced with the participation of deep-seated fluids.

## INTRODUCTION

The Megradzor deposit in Armenia offers a very interesting example of gold deposits in young volcano-plutonic belts of the Mediterranean Province. In addition to features typical of epithermal deposits (the presence of telluride mineralization, crustification structures, and other textural and structural features of ores that are suggestive of their deposition in open cracks), mineralization at this deposit displays apparent spatial and genetic links with magmatic bodies and other indications of relationships with deep-seated processes. Features of this type can also be identified during detailed study of other deposits and testify to the involvement of diverse sources of mineralizing fluids and ore material. Taking into account these facts and considerations, we undertook a further study (our earlier results were published in [1]) of the mineralizing fluids and genetic conditions responsible for the origin of mineral assemblage diversity, primarily, early hydrothermal mineralization, with the aim to constrain the physicochemical parameters and determine the composition of fluids of different geneses that took part in the formation of the Megradzor deposit.

## GEOLOGY OF THE DEPOSIT AND ITS ORES

The Megradzor deposit in Armenia is located in the zone of the Ankavan deep fault, which separates the Pambak and Tsakhkunyan tectono-stratigraphic zones of the Lesser Caucasus. The basement of the geologic sequence is composed of rocks of a pre-Paleozoic metamorphic complex (quartz–mica schists, greenschists, and amphibolites) and Jurassic plagiogranite, which cuts all of these rocks. These are conformably overlain by a Paleogene volcano-sedimentary sequence, which is approximately three kilometers thick and consists of variably propylitized andesites, basaltic andesites, andesite-dacites, trachyandesites, trachydacites, and, more rarely, their lava- and tuff-breccias, tuffites, and tuff-sandstones. The stratigraphic section of the deposit is crowned by a compositionally diverse Pliocene succession of continental volcanics up to 400 m in thickness. The succession contains abundant bodies of post-Late Eocene–pre-Miocene granodiorite, granosyenite, syenite, and monzonite and granosyenite porphyry, diabase, diorite porphyry, and micaceous lamprophyre dikes. At contacts with the granitoids, the rocks of the Paleogene volcanic sedimentary sequence are transformed to hornfels within a zone from a few to a few dozen meters in thickness.

Relatively thin (0.2–0.8 m and up to 2–3 m in swells) gold-bearing quartz, sulfide–quartz, and sulfide–telluride–quartz veins usually dip at high angles (45°–80°) and are hosted by the zone of the regional Ankavan fault, within which they are spatially restricted to splay east-striking fractures and are localized within extensively tectonized linear zones of argillisites–beresites. Along their dips and strikes, the veins often grade into vein zones, which, in turn, often give way to disseminated and stringer mineralization [2–4].

Some orebodies (I, II, and Slepoe) are closely associated with steeply dipping micaceous lamprophyre dikes, which are often conformable with the dips and strikes of the ore-hosting fractures and contain ore mineralization [5]. Orebodies I and II are hosted only by volcanic rocks, orebodies IX and Slepoe are partly contained by volcanics and partly by intrusive rocks, and others (for example, orebody VI) are fully enclosed in intrusive rocks. The overall known vertical magnitude of the gold mineralization is 300–350 m.

A genetically very interesting skarn body, which was discovered during the prospecting of deep levels of the western flank of the Central Prospect between orebodies II and Slepoe, is dominated by magnetite. It is localized diagonally (at angles of 50°–70°) with respect to gold orebodies and extends along the outer contact zone of a dike-shaped granosyenite intrusion in propylitized and weakly hornfelsed rocks of the lower part of the Paleogene sequence. The skarn is accompanied by intense epidotization. The absence of direct relations between the iron and gold mineralization and the lack of evidence of genetic links between them, the localization of the magnetite skarn in a structure unfavorable for gold mineralization, and the distinct types of the wall-rock alterations point to different geneses of the two mineralization types. The fact that the gold grade of the magnetite skarn ore increases from virtually zero to 0.3–0.5 g/t in areas with overprinted quartz–sulfide mineralization indicates that the iron mineralization is older than the gold mineralization.

The gold mineralization includes more than 40 hypogene ore minerals [2, 4, 6, 7], the main of which are pyrite, chalcopyrite, galena, sphalerite, and compositionally variable fahlore of the goldfieldite–tennantite–tetrahedrite series. In places, orebodies are high in numerous compounds of Te with Au, Ag, Bi, Pb, Ni, Hg, and other elements (calaverite, krennerite, sylvanite, petzite, nagyagite, buckhornite, hessite, stutzite, empressite, coloradoite, altaite, melonite, tellurobismuthite, tetradymite, and others). Pyrrhotite, marcasite, luzonite, enargite, bornite, chalcosine, and Bi sulfosalts (bismuthite, aikinite, and wittechinite) were encountered in orebodies in small amounts but not ubiquitously. However, the magnetite skarn body bears bornite, chalcosine, and covellite as its main sulfide minerals. The most widespread gangue mineral of the gold orebodies is quartz (60–90 vol %), and the base-metal sulfides and tellurides are associated with significant amounts of carbonates, mainly Mn-calcite and dolomite.

The observable spatial and age relations between mineral assemblages of both the gold–sulfide–telluride–quartz ores of the Megradzor and the iron skarn mineralization suggest that the deposit contains coexisting products of distinct stages of the postmagmatic process: high-temperature skarns and hydrothermal gold mineralization proper (Table 1). Taking into account the results of earlier research [2, 3], we subdivided the genesis of the hydrothermal gold mineralization into five periods or stages [6], four of which produced ore mineralization [quartz–pyrite–hematite (I), quartz–chalcopyrite–pyrite (II), gold–galena–sphalerite (III), gold–silver–telluride (IV)] and one of which [quartz–carbonate (V)] is a postmineralization stage (Table 1).

The distribution of the gold–sulfide–telluride mineralization over the vertical section of individual orebodies show apparent zoning [7]. At the lowermost levels (with elevations below +1950 m above sea level; adits 9, 10, 13, 21, 40, 100, 102, 103, Transportnaya, and others), ore mineralization occurs mainly as relatively thin veins, stringers, and pockets of quartz and sulfide–quartz ores. The sulfide segregations usually consist of pyrite and chalcopyrite, sometimes of chalcopyrite and tennantite or chalcopyrite, bornite, and enargite. The ore and gangue minerals are usually intensely cataclazed and, in places, are cemented with quartz–carbonate–sphalerite–galena aggregates. The ores and veins sporadically bear small pockets and veinlets of quartz–carbonate–telluride composition, which are discordant relative to sulfide aggregates.

At the upper levels of the orebodies (with elevations of more than +1950 m above sea level; adits 6, 7, 20, 27, 50, 70, 101, 104, 106, 108, and others), the ores are dominated by assemblages of base-metal sulfides, fahlores, tellurides, and Bi sulfosalts. However, some ore bodies contain, along with these minerals, significant concentrations of pyrite and chalcopyrite. Telluride pockets and stringers are restricted to both pyrite–chalcopyrite and sphalerite–galena aggregates and are always anhedral with respect to them. At the same time, carbonate–telluride segregations sometimes occur enclosed in quartz with no apparent connection with the sulfide mineralization.

The latest minerals at the deposit are thin veins and veinlets of fine-grained, chalcedonic quartz and carbonates of stage V, which cut across mineral aggregates of all mineralization stages and occur ubiquitously at the lower and upper levels of orebodies.

Gold, the principal commercial component of the Megradzor ores, occurs as a native metal and a diversity of tellurides (calaverite, krennerite, sylvanite, petzite, nagyagite, and buckhornite). The native gold commonly develops as small (0.1–0.3 mm) blebs, platelets, amoeba-shaped particles, and veinlets, which are gen-

**Table 1.** Scheme of the crystallization succession of minerals and their relative abundances in the ores of the Megradzor deposit

| Mineralizing phase and stage | Skarn with iron mineralization | | | Hydrothermal with gold mineralization | | | | |
|---|---|---|---|---|---|---|---|---|
| | garnet–epidote–quartz | mushketovite–magnetite | epidote–pyrite–chalcopyrite | quartz–hematite–pyrite (I) | quartz–chalcopyrite–pyrite (II) | gold–galena–sphalerite (III) | gold–silver–telluride (IV) | quartz–carbonate (V) |
| Garnet | ++++ | ++ | | | | | | |
| Epidote | ++++ | ++++ | +++ | | | | | |
| Sphene | | + | | | | | | |
| Apatite | | + | | | | | | |
| Actinolite | | ++ | | | | | | |
| Quartz | +++ | +++ | ++ | ++++ | ++++ | +++ | +++ | +++ |
| Carbonates | ++ | ++ | ++ | + | ++ | + | ++ | ++++ |
| Chlorite | | + | ++ | ++ | ++ | ++ | | |
| Sericite | | | | + | ++++ | +++ | + | |
| Montmorillonite | | | | ++++ | ++ | ++ | ++ | |
| Kaolinite and dickite | | | | | | ++ | ++ | |
| Magnetite | +++ | ++++ | | | | | | |
| Mushketovite | | +++ | | | | | | |
| Hematite | | + | + | +++ | | | | |
| Pyrite | | ++ | ++++ | ++++ | ++++ | ++ | ++ | ++ |
| Marcasite | | | | + | ++ | ++ | | + |
| Pyrrhotite | | | | + | | | | |
| Bornite | | + | | | ++ | | | |
| Chalcocite | | + | | | | | | |
| Chalcopyrite | | + | +++ | + | ++++ | +++ | ++ | |
| Enargite | | | | | ++ | | | |
| Luzonite | | | | | +++ | | | |
| Tennantite | | | | + | ++ | +++ | | |
| Tetrahedrite | | | | | | ++ | | |
| Goldfieldite | | | | | | + | | |
| Sphalerite | | | | | ++ | ++++ | + | |
| Galena | | | | | ++ | ++++ | +++ | |
| Bi sulfosalts | | | | | + | | | |
| Altaite | | | | | | + | +++ | |
| Coloradoite | | | | | | | ++ | |
| Tellurobismuthite | | | | | | | + | |
| Tetradymite | | | | | | + | ++ | |
| Calaverite | | | | | | + | ++ | |
| Krennerite | | | | | | | ++ | |
| Buckhornite | | | | | | | + | |
| Nagiagite | | | | | | | + | |
| Sylvanite | | | | | | | +++ | |
| Petzite | | | | | | | ++ | |
| Hessite | | | | | | + | +++ | |
| Stutzite | | | | | | + | ++ | |
| Empressite | | | | | | | ++ | |
| Native gold | | | | | + | +++ | ++ | |
| Native tellurium | | | | | | | ++ | |

Note: Relative abundances of minerals: ++++ predominant, +++ typical, ++ subordinate, + trace.

erally associated with minerals of the gold–galena–sphalerite stage (stage III) and those of the gold–silver–telluride stage (stage IV). The fineness of the gold is generally high (>890), and only gold specks of the late silver–telluride association of stage IV are 810–820 fine [6].

## SAMPLES AND METHODS

In order to reveal the regularities in the *P–T* evolution of the hydrothermal solution and its chemical, gas, and isotopic composition during the development of gold mineralization at the Megradzor deposit, we used a collection of representative samples from the main orebodies (I, II, VI, IX, XIV, and Slepoe). For comparison, we also examined samples of the barren magnetite skarn body which predated the deposition of the gold mineralization.

The gold orebodies in question are veins, lenses, and zones of stringer and disseminated mineralization spatially restricted to relatively gently dipping structures of roughly eastern and northeastern strikes. As can be seen from Table 2, orebody Slepoe is most fully characterized by samples and was studied over a depth interval from +1820 m (adit 100) to +2065 m (adit 104). Samples from orebody I were collected only in its upper part, and those from orebodies II, VI, IX, and XIV are from their deep levels (Table 2). The samples made it possible to reveal regularities in the evolution of the mineralizing solution starting from earlier to later stages of the gold-forming mineralizing process.

The complex of techniques utilized in our research included thermo- and cryometry of individual fluid inclusions (FI) in quartz, ion and gas chromatographic analyses of FI, neutron-activation and atomic-absorption analyses with the purpose of determining the concentrations of gold and other metals in FI, and mass spectrometric determination of the oxygen isotopic composition of quartz and the sulfur isotopic composition of sulfides.

**Thermo- and cryometry of fluid inclusions.** Individual FI in quartz of several distinct generations were examined in polished platelets 0.3–0.5 mm in thickness. The homogenization temperatures, $T_h$, were determined in a heating–freezing stage designed by V.A. Kalyuzhnyi with the use of long-focus objectives with magnifications of 40, 22, and 16x. The accuracy of the $T_h$ determinations was ±2°C. Our cryometric studies were conducted in a stage designed by V.A. Simonov, with liquid nitrogen serving as the cooling agent and temperature controlled by a standardized Chromel–Alumel thermocouple. The melting temperatures of eutectics, $T_e$, were determined accurate to ±1.5°C; the $CO_2$ melting points, $T_{m,CO_2}$, were determined accurate to ±0.5°C; and the melting points of ice, $T_m$, gas hydrates, $T_{m,gh}$, and the homogenization temperatures of $CO_2$, $T_{h,CO_2}$, were determined accurate to ±0.2°C. The concentrations of salts in two-phase inclusions were calculated (as equivalent NaCl concentrations) using data from [8, 9]. The concentrations of salts in aqueous carbon dioxide inclusions were assayed from the melting points of the gas hydrates and recalculated to $H_2O$–$CO_2$–NaCl [10]. When concentrations of $CO_2$ in individual FI were high, they were calculated based on measured volumetric phase proportions with the use cryometric data.

The pressure was evaluated based on syngenetic gas-dominated and gas–liquid inclusions, which were captured during fluid homogenization, and based on inclusions of saturated solutions, in which a halite crystal dissolved after homogenization of the gas bubble [11]. In the former case, the pressure was evaluated with the FLINCOR (version 1.21) computer program [12], with $CO_2$ isochores calculated by the equations from [13]. In the latter case, analogous values were deduced from generalized experimental data on the densities of NaCl solutions at elevated temperatures and pressures [14]. In both cases, the values thus obtained were added to the saturated vapor pressures, which were calculated with the use of data from [15].

**Gas and ion chromatography.** The samples of quartz fractions (–1.0 + 0.5 mm), which were carefully hand-picked under a binocular magnifier, were treated by hot $HNO_3$ (1 : 1), washed with distilled and, then, twice-distilled water, and dried at temperatures of 100–120°C. Samples (300 mg) were put into the furnace of a chromatograph and held in a helium flow for 20–30 min at 120°C. The thermal opening of the quartz was carried out at 450°C. The composition of volatiles ($H_2O$, $CO_2$, $CH_4$, and others), cations ($Na^+$ and $K^+$), and anions ($Cl^-$, $F^-$, and $SO_4^{2-}$) was determined by the methods designed at the Vernadsky Institute of Geochemistry and Analytical Chemistry, Russian Academy of Sciences, and was described in detail in [16, 17].

Sulfide sulfur was analyzed potentiometrically by a sulfide–silver electrode [18]. All measurements were carried out in a box through which purified $O_2$, $CO_2$, and Ar flows were continuously passed. A 2-g quartz sample in a jasper mortar was put into the box. After grinding the sample in an alkali solution for 1 h, the above sample solution was taken for analysis of the sulfide sulfur concentration. The sensitivity of the method was $10^{-6}$ M total sulfur concentration; the analytical error was ±10%.

**Mass spectrometric determinations of oxygen and sulfur isotopic compositions.** The O and S isotopic composition of sulfides from Megradzor ores was determined at the Laboratory of Isotopic Geochemistry and Geochronology of the Institute of the Geology of Ore Deposits, Petrography, Mineralogy, and Geochemistry, Russian Academy of Sciences, in compliance with the conventional technique described in [19].

**Table 2.** Characteristics of ore samples from the Megradzor deposits and analytical techniques utilized in their examination

| Sample | Orebody | Elevation, m | Sampling site | Note | Analytical techniques | | | | | | | |
|---|---|---|---|---|---|---|---|---|---|---|---|---|
| | | | | | t + c | ich | gch | $S_2$ | $Au^+$ | $Cu^+$ | $\delta^{18}O$ | $\delta^{34}S$ |
| 148/87 | I | +2135 | adit 70 raise 2 | Sulfide–quartz vein | + | + | + | | | | + | + |
| 79/87 | I | +2080 | adit 7 bl. 3/13 | Sulfide–telluride–quartz vein, Au-rich (up to 10 g/t) ore shoot | + | + | + | | + | | + | + |
| 65/87 | Slepoe | +2065 | adit 104, ore drive | Carbonate and quartz masses in the upper part of the orebody | + | + | + | | + | | + | |
| 108/87 | Slepoe | +2040 | adit 101, drive 2 | Sulfide–telluride–quartz vein | + | + | + | + | + | | + | |
| 109/87 | Slepoe | +2040 | adit 101, drive 2 | Sulfide–telluride–quartz vein | + | + | + | + | + | | + | |
| 133/87 | Slepoe | +2040 | adit 101, drive 2 | Sulfide–telluride–quartz vein | + | | | | | | | |
| 88/87 | Slepoe | +1923 | adit 40, shaft | Sulfide–quartz vein | + | | | | | | | |
| 128/87 | Slepoe | +1923 | adit 101, drive 2 | Sulfide–telluride–quartz vein | + | + | + | | + | | + | |
| 434/87 | II | 1820 | adit 10', shaft | Sulfide–quartz vein, Au-rich (up to 40–60 g/t) ore shoot | + | | | | | | | |
| MD-392 | II | +1820 | adit 100, shaft | Sulfide–quartz vein | + | | | | | + | | |
| MD-394 | II | +1820 | adit 100, shaft | Sulfide–telluride–quartz vein | + | | | | | | | |
| 110/87 | VI | +1820 | adit 100, drive 2b | Sulfide–telluride–quartz vein | + | + | + | | + | | + | + |
| 112/87 | VI | +1820 | adit 100, drive 2b | Sulfide–quartz vein | + | + | + | | + | + | + | + |
| 119/87 | VI | +1820 | adit 100, drive 2b | Sulfide–telluride–quartz vein | + | + | + | | + | + | + | |
| 135/87 | VI | +1820 | adit 100, drive 6 | Sulfide–quartz vein | + | + | + | + | + | + | + | |
| 139/87 | IX | +1820 | adit 100, shaft | Sulfide–quartz vein | + | | + | | | + | + | + |
| 454/90 | XIVA | +1820 | adit 10, shaft | Sulfide–quartz vein, Au-rich (up to 50 g/t) ore shoot | | + | | | | | | |
| 454a/90 | XIVA | +1820 | adit 10, shaft | Sulfide–quartz vein, Au-rich (up to 80 g/t) ore shoot | | + | | | | | | |
| 136/87 | Slepoe | +1820 | adit 100, drive 2 | Sulfide–telluride–quartz vein | | + | | | | | + | |
| MD-64 | Slepoe | +1820 | adit 100, shaft | Sulfide–telluride–quartz vein | | + | | | | | | |
| 448/90 | Slepoe | +1820 | adit 100, crosscut 2 drive 4 | Sulfide–quartz vein | | + | | | | | | |
| 351/90 | Slepoe | +1820 | adit 100, drive 5 | Sulfide–quartz vein with chalcopyrite–pyrite (up to 10 g/t Au) and sphalerite–galena (20–30 g/t Au) mineralization | | + | | | | | | |
| 402/90 | Slepoe | +1820 | adit 100, drive 5 | Veinlet of premineralization amethysthic quartz | | + | | | | | | |
| 3210/90 | Slepoe | +1820 | adit 100, drive 5 | Quartz-dominated mineralization with hematite and sulfides | | + | | | | | | |
| MD-10a | | +1820 | adit 100, shaft | Magnetite skarn body | | + | | | | | | |
| M-10 | | +1820 | adit 100, shaft | Gypsum pocket among tuffizites | | + | | | | | | |

Note: Methods: t + c—thermo- and cryometry of individual fluid inclusions; ich—ion chromatography; gch—gas chromatography; $S_2$—sulfide sulfur concentration; $Au^+$—bulk Au, Te, Sb, and As concentrations determined in fluid inclusions; $Cu^+$—Cu, Fe, Mn, Zn, and Sn concentrations determined in individual fluid inclusions; $\delta^{18}O$—oxygen isotopic composition of quartz; $\delta^{34}S$—sulfur isotopic composition of sulfides.

Quartz and sulfide fractions (–0.5 + 0.25 mm) were carefully hand-picked under a binocular magnifier.

## RESULTS OBTAINED ON FLUID INCLUSIONS AND THEIR DISCUSSION

**Thermo- and cryometry of individual FI.** During the visual study of transparent polished platelets under an optical microscope, we determined that the quartz contains numerous FI. Apparently, primary FI were encountered in two samples, in which they were restricted to growth zones in quartz grains. Most inclusions are equally distributed over the volumes of the host minerals or are arranged along cracks, which do not extend outside the crystal, and are most probably pseudosecondary. These inclusions are commonly shaped as negative crystals from 3 to 25 μm in size (mainly, 10–15 μm), whereas secondary FI are usually anhedral with respect to quartz and range from 5 to 40 μm.

In accordance with their phase composition, the FI detected in quartz from the Megradzor deposit can be classified into four types. (1) Polyphase inclusions of chloride brines with two–three or more optically isotropic crystals, aqueous solution, and a gas bubble. These inclusions were encountered only in quartz samples from the magnetite skarn body. (2) Three-phase aqueous carbon dioxide FI, which contain aqueous solution, liquid carbon dioxide, and a bubble of gaseous carbon dioxide. (3) Three-phase carbon dioxide FI, which are syngenetic with the inclusions of type 2 and contain liquid and gaseous carbon dioxide and a small meniscus of aqueous solution. The inclusions of types 2 and 3 are mostly primary and pseudosecondary and are usually hosted by quartz of early (I and II) stages of the gold-mineralizing process. (4) Two-phase primary, pseudosecondary, and secondary gas–liquid FI, which were encountered in quartz of all of the gold-mineralization stages and contained aqueous solution and a gas ($H_2O$ and $CO_2$) bubble.

Our thermo- and cryometric results obtained on 567 individual FI in 26 samples are summarized in Table 3 and graphically presented in a series of diagrams in Fig. 1. We are aware that the classification of inclusions with certain stages seems to have been not always fully reliable; nevertheless, our results revealed certain regularities in the variations of the physicochemical parameters that reflect the compositional evolution of the mineralizing fluids and genetic mineralization conditions. Inclusions of later generations may sometimes be contained in quartz of earlier association but not vice versa. Because of this and in spite of the "interference effect" of some deviating data, the general situation can be unraveled clearly enough by analyzing a large body of data on individual FI. Moreover, we sometimes even managed to identify evidence of the relative age of discrete inclusion groups (in particular, when brine inclusions were refilled with aqueous carbon dioxide fluid, as in Sample MD-10a; this fact led us to class these inclusions with the first mineralization stage but not with the skarn stage, analogously with the identification of discrete inclusion groups in Sample 454/90 and some others). As can be seen, the parameters calculated for virtually all of the samples are spread over fairly broad intervals of values. For the convenience of using these data, all of the parameters are made consistent with the $T_h$ values, whose intervals are listed in Table 3 beginning from the highest value. Evidently, the parameters and composition of the fluid varied both within a single stage and with the transition between discrete stages. While the variations in the physicochemical parameters of a single stage can be explained by evolutionary changes, the transitions between the associations of different stages (for example, from the skarn stage to stage I or from stage III to stage IV) were most probably related to changes in the tectonic environments and the inflow of fluid of different chemistry into the system.

Our data (Table 3) demonstrate that the solutions that produced the gold-free magnetite-skarn mineralization during the postmagmatic iron-mineralization stage had *P–T* characteristics and a composition notably different from those of the fluids from which the gold mineralization was deposited. These high-salinity solutions (55.2–34.7 wt % equiv. NaCl) had a chloride–calcic composition ($T_e$ from –54 to –55°C) and high pressures (up to 2270 bar) at relatively high temperatures (465–250°C). High pressures are also evident from the decrepitation of most of these inclusions during heating, so that only a few of the smallest inclusions could be heated to temperatures sufficient for their homogenization. High pressures (2180–470 bar) and medium temperatures (360–271°C) were determined for inclusions of heterogeneous solutions which had different cationic–anionic compositions ($T_e$ from –41 to –33°C), different salt concentrations (11.8–1.8 wt % equiv. NaCl), and produced the early quartz–pyrite–hematite mineralization of stage I of the gold-mineralization stage. This mineralization developed at deep levels of the deposit. The inclusions were rich in carbon dioxide (5.7–2.3 mol/kg of $H_2O$). They also actively decrepitated when heated, so that only a few of them could be homogenized. The pressures (and, partly, temperatures) of the skarn association and the association of stage I differ from the typical parameters of epithermal gold deposits and approach those of the mesothermal type.

The mineral assemblages of the early productive quartz–chalcopyrite–pyrite stage (II) were deposited by a $CO_2$-rich (up to 5.0 mol/kg of $H_2O$) Cl–Mg–Na ($T_e$ from –37 to –28°C) solution of moderate salinity (7.5–1.4 wt % equiv. NaCl) at moderate temperatures (328–202°C) and pressures (590–180 bar) simultaneously with frequent episodes of fluid heterogenization. This stage can be regarded as transitional to the associations of stages III and IV and displays similarities with both meso- and epithermal deposits.

In one of our samples of the quartz–chalcopyrite–pyrite associations, a gas inclusion with liquid $CO_2$ was

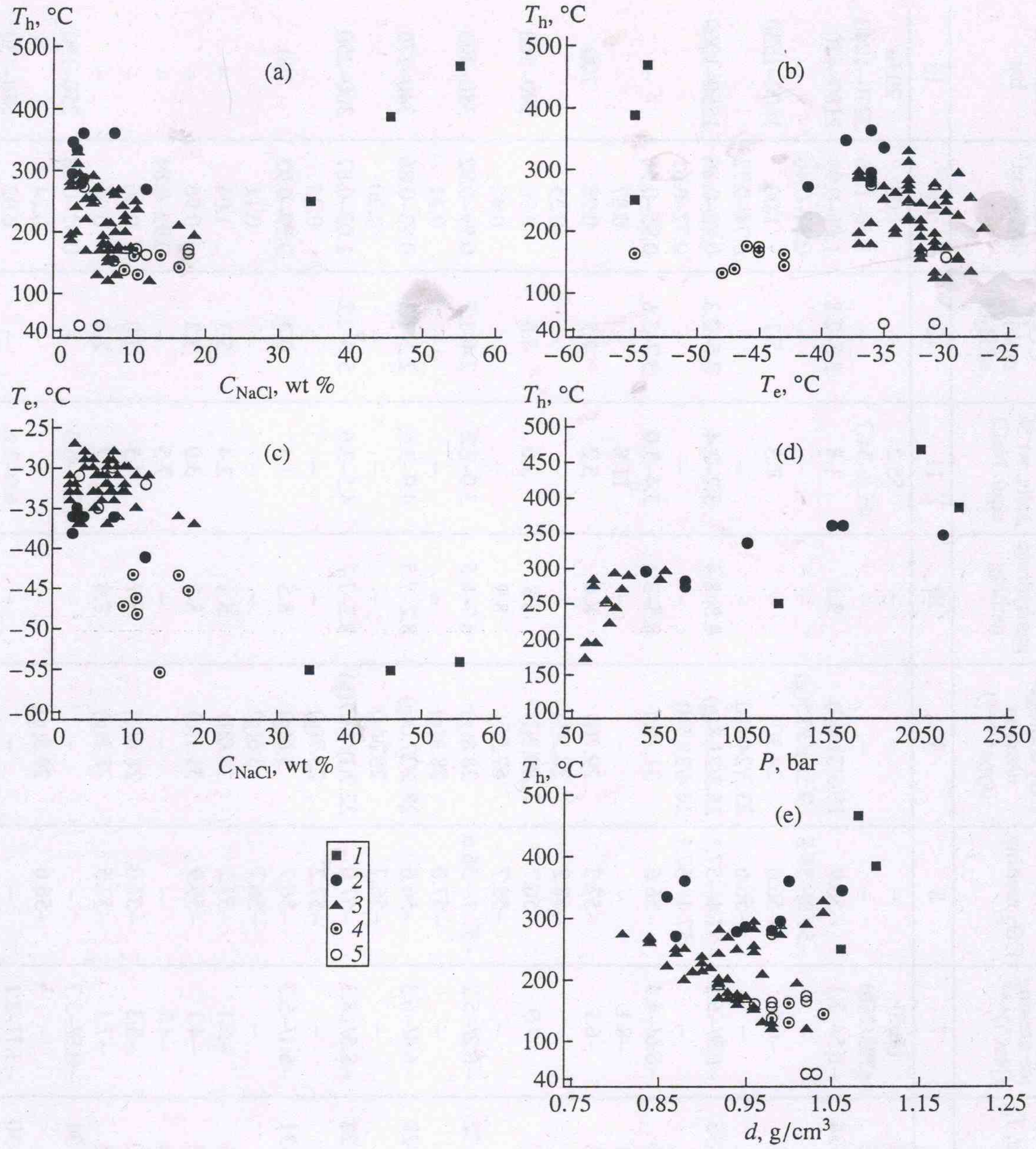


**Fig. 1.** Diagrams (a) homogenization temperature–salt concentrations, (b) homogenization temperature–eutectic temperature, (c) eutectic temperature–salt concentrations, (d) homogenization temperature–pressure, and (e) homogenization temperature–fluid density based on results obtained by thermo- and cryometric techniques on individual fluid inclusions in quartz of the main stages (mineral assemblages of ores) at the Megradzor deposit.

(*1–5*) Mineralization stages: (*1*) mushketovite–magnetite skarn, (*2*) quartz–magnetite–pyrite, (*3*) quartz–chalcopyrite–pyrite, (*4*) gold–galena–sphalerite, (*5*) gold–silver–telluride. Each row of Table 3 corresponds to two points (minimum and maximum values, when an interval of parameters is cited) or a single point (when only one value was determined).

detected to contain a significant admixture of $H_2S$ ($T_{h,\,CO_2}$ increased to +67.5°C), similarly to the inclusions described in [20]. The $H_2S$ concentration of the hydrothermal solution seems to have been fairly high during the early stages, as was also earlier mentioned for the mineralizing fluid at the Megradzor deposit in [21, 22].

Our data (Tables 3, 4) demonstrate that the mineralizing solutions of the early (I, II) stages had several parameters, first of all, pressure, concentration of dissolved gases, and temperatures, which were remarkably different from those of typical epithermal fluids that produced gold deposits [23]. At the same time, the Megradzor fluids exhibit certain similarities with $CO_2$-enriched solutions that produced some mesothermal gold deposits in terrigenous sequences. Our newly obtained data on pressure indicate that both the magnetite skarn and the quartz–hematite–pyrite mineraliza-

**Table 3.** Microthermometric data on individual fluid inclusions in quartz from mineralized veins at the Megradzor deposit, Armenia

| Sample | Stage* | *n*** | Temperature, °C | | | | | | Concentration | | Fluid density, g/cm$^3$ | Pressure, bar |
|---|---|---|---|---|---|---|---|---|---|---|---|---|
| | | | homogenization (gas disappearance, $T_h$) | eutectic, $T_e$ | ice melting (NaCl)*** | $CO_2$ melting | $CO_2$ homogenization (type****) | gas hydrate melting | salts, wt % equi. NaCl | $CO_2$, mol/kg of $H_2O$ | | |
| 1 | 2 | 4 | 5 | 6 | 7 | 8 | 9 | 10 | 11 | 12 | 14 | 15 |
| MD-10a | MS | 8 | 314 | –54 | **(465)** | – | – | – | 55.2 | – | 1.08 | 2050 |
| Same | MS | 29 | 192–141 | –55 | **(385/250)** | – | – | – | 45.8–34.7 | – | 1.10–1.06 | 2270–1240 |
| 402/90 | I | 7⊗ | 345–294 | –38/–36 | –8.5/–7.1 | –56.9 | 10.5/31.0(l) | 9.1 | 1.8 | 5.5–2.8 | 1.06–0.99 | 2180–470 |
| Same | I | 23⊗ | – | – | – | –56.9/–56.8 | 9.5(l)/30.5(g) | – | – | – | 0.87–0.40 | |
| 454/90 | I | 3⊗ | 360 | –36 | –6.6 | –56.6 | 24.3(l) | – | 7.5 | 5.7 | 1.00 | 1600–1530 |
| Same | I | 5⊗ | – | – | – | –56.6 | 23.3/24.4(l) | – | – | – | 0.74–0.72 | |
| 351/90 | I | 5⊗ | 360–335 | –36/–35 | –6.9/–6.2 | –57.4/–57.1 | 26.3/21.8(g) | 8.8–8.4 | 3.2–2.4 | 2.5–2.3 | 0.88–0.86 | 1550–1060 |
| Same | I | 18⊗ | – | – | – | –57.4/–57.1 | 24.4/29.5(l) | – | – | – | 0.72–0.61 | |
| MD-10a | I | 9 | 288–279 | –36 | –6.6/–4.4 | –56.6 | 31.1(c) | 8.5–8.3 | 3.4–3.0 | 3.7–3.6 | 0.95–0.94 | – |
| Same | I | 12 | 271 | –41 | –8.1 | – | – | – | 11.8 | – | 0.87 | – |
| 434/90 | I | 4⊗ | 281–274 | –36 | –6.1 | –57.2 | 29.7(l) | 8.4 | 3.2 | 4.5 | 0.98 | 700 |
| Same | I | 3⊗ | – | – | – | –58.2 | 28.5(l) | – | – | – | 0.55 | |
| 454a/90 | II | 6⊗ | 295–283 | –37 | –7.9 | –56.7 | 7.2/9.3(l) | 8.9 | 2.6 | 4.6 | 0.96 | 590–560 |
| Same | II | 2⊗ | – | – | – | –58.7 | 67.5(l) | 8.9 | – | – | 0.45 | |
| 112/87 | II | 6⊗ | 288–242 | –37/–32 | –6.2/–5.2 | –57.1/–56.6 | 28.8(g) | 8.9–8.5 | 3.0–2.2 | 2.4–1.7 | 0.99–0.92 | 380–300 |
| Same | II | 4⊗ | – | – | – | –57.0 | 28.8(g) | – | – | – | 0.31 | |
| 110/87 | II | 7⊗ | 270–221 | –35/–29 | –6.4/–6.3 | –56.6 | 28.3/27.0(g) | 8.2–7.5 | 4.9–3.6 | 2.2–1.3 | 0.93–0.86 | 340–270 |
| Same | II | 4⊗ | – | – | – | –56.7 | 28.3(g) | – | – | – | 0.30 | |
| 135/87 | II | 11⊗ | 291–252 | –29/–28 | –8.5/–8.3 | –57.0 | 22.9(l)/23.7(g) | 8.2–7.7 | 4.5–3.6 | 5.0–2.2 | 1.02–0.87 | 300–250 |
| Same | II | 3⊗ | – | – | – | –57.2 | 23.7(g) | – | – | – | 0.23 | |
| 119/87 | II | 4⊗ | 282–274 | –33/–31 | –6.1/–5.3 | –56.7 | 3.6(g) | 8.5 | 1.4 | 0.9 | 0.99–0.92 | 180 |
| Same | II | 3⊗ | – | – | – | –56.7 | 3.6(g) | – | – | – | 0.11 | |
| 3210/90 | II | 3 | 328–309 | –33 | –5.1 | –57.2 | 14.0(l) | 8.8 | 2.4 | 5.3 | 1.04 | – |
| 119/87 | II | 5 | 255–244 | –33 | –4.1 | –56.9 | 31.1(c) | 8.5 | 3.0 | 3.2 | 0.96 | – |
| 136/87 | II | 3 | 260–202 | –34 | –4.7 | – | – | – | 7.5 | – | 0.92–0.84 | – |
| 128/87 | II | 3 | 255–245 | –30 | –8.3 | –57.0 | 28.6(g) | 7.7 | 4.5 | 2.0 | 0.96 | – |
| 351/90 | II | 3 | 249 | –33 | –7.1 | –57.5 | 28.2(g) | 7.6 | 4.7 | 2.3 | 0.94 | – |
| MD-392 | III | 8⊗ | 250–194 | –35/–31 | –6.9/–3.7 | – | – | – | 10.4–6.0 | – | 0.92–0.88 | 250–190 |
| Same | III | 5⊗ | – | – | – | –56.6 | 24.5(g) | – | – | – | 0.24 | |
| MD-394 | III | 7⊗ | 194–172 | –34/–30 | –3.7/–2.1 | – | – | – | 6.0–3.6 | – | 0.92 | 140–130 |
| Same | III | 3⊗ | – | – | – | –56.6 | 15.7(g) | 8.5 | – | – | 0.16 | |

**Table 3.** (Contd.)

| 1 | 2 | 4 | 5 | 6 | 7 | 8 | 9 | 10 | 11 | 12 | 14 | 15 |
|---|---|---|---|---|---|---|---|---|---|---|---|---|
| 119/87 | III | 10 | 197–189 | –34/–32 | –4.2/–3.4 | –56.7/–56.6 | N.a. | 8.5 | 1.4 | N.a. | 0.92 | – |
| 351/90 | III | 8 | 272 | –33 | –3.2 | – | – | – | 5.3 | – | 0.81 | – |
| Same | III | 22 | 213–181 | –32/–31 | –3.9/–3.6 | – | – | – | 6.3–5.9 | – | 0.93–0.89 | – |
| MD-64 | III | 11 | 269–201 | –31/–27 | –5.1/–1.3 | – | – | – | 8.0–2.2 | – | 0.88–0.84 | – |
| 88/87 | III | 11 | 268–201 | –31/–27 | –5.1/–1.3 | – | – | – | 8.0–2.2 | – | 0.88–0.84 | – |
| 139/87 | III | 13 | 264–215 | –33 | –4.6/–4.4 | – | – | – | 7.3–7.0 | – | 0.90–0.84 | – |
| Same | III | 3 | 121 | –31 | –8.4 | – | – | – | 12.2 | – | 1.02 | – |
| 454a/90 | III | 17 | 244 | –33 | –5.6 | – | – | – | 8.7 | – | 0.87 | – |
| Same | III | 8 | 210 | –36 | –12.5 | – | – | – | 16.4 | – | 0.97 | – |
| " | III | 11 | 152 | –32 | –4.0 | – | – | – | 6.5 | – | 0.96 | – |
| 148/87 | III | 6 | 238–174 | –31/–30 | –7.1/–6.3 | – | – | – | 10.6–9.6 | – | 0.95–0.90 | – |
| 135/87 | III | 15 | 228–170 | –30 | –5.9/–4.9 | – | – | – | 9.1–7.7 | – | 0.94–0.90 | – |
| 133/87 | III | 27 | 220–152 | –33/–29 | –5.9/–4.4 | – | – | – | 9.1–7.0 | – | 0.96–0.91 | – |
| 110/87 | III | 4 | 202–156 | –32/–29 | –5.8/–4.6 | – | – | – | 9.0–7.3 | – | 0.96–0.93 | – |
| 454/90 | III | 18 | 196–177 | –37 | –14.8/–4.1 | – | – | – | 18.5–6.6 | – | 1.01–0.94 | – |
| 3210/90 | III | 28 | 180–171 | –31 | –4.0/–3.2 | – | – | – | 6.5–5.3 | – | 0.93 | – |
| 136/87 | III | 13 | 178–121 | –36/–30 | –5.1/–4.1 | – | – | – | 8.0–6.6 | – | 0.98–0.94 | – |
| 128/87 | III | 14 | 169–131 | –30/–28 | –5.8/–4.9 | – | – | – | 9.0–7.7 | – | 0.98–0.95 | – |
| 434/90 | III | 21 | 169 | –32 | –4.2 | – | – | – | 6.7 | – | 0.94 | – |
| 448/90 | III | 21 | 160–132 | –32/–31 | –4.1/–3.1 | – | – | – | 6.6–5.1 | – | 0.97–0.94 | – |
| 108/87 | III | 10 | 156–147 | –33/–30 | –8.2/–6.1 | – | – | – | 11.9–9.3 | – | 0.99–0.96 | – |
| Same | IV | 3 | 175–168 | –45 | –13.9 | – | – | – | 17.7 | – | 1.02 | – |
| 79/87 | IV | 5 | 175–163 | –46/–43 | –7.1/–6.8 | – | – | – | 10.6–10.2 | – | 0.96–0.94 | – |
| 136/87 | IV | 6 | 164–132 | –55/–48 | –10.0/–7.2 | – | – | – | 13.9–10.7 | – | 1.00 | – |
| 133/87 | IV | 2 | 144 | –43 | –12.5 | – | – | – | 16.4 | – | 1.04 | – |
| MD-64 | IV | 4 | 139 | –47 | –5.7 | – | – | – | 8.8 | – | 0.98 | – |
| 65/87 | V | 19 | 165–122 | –32/–30 | –8.1/–4.6 | – | – | – | 11.8–7.3 | – | 0.98 | – |
| M-10 | V | 8 | <50 | –35/–31 | –3.2/–1.6 | – | – | – | 5.3–2.7 | – | 1.03–1.02 | – |

Notes: * Mineralization stages: MS—magnetite skarn, I—premineralization quartz–pyrite–hematite, II—quartz–chalcopyrite–pyrite, III—gold–galena–sphalerite, IV—gold–silver–telluride, V—postmineralization quartz–chalcedony–carbonate.

** Numbers of inclusions examined. ⊗—Heterogeneous fluid.

*** Numbers in parentheses denote halite dissolution temperature.

**** Types of $CO_2$ homogenization: g—into gas, l—into liquid, c—with critical phenomena. In Sample M-10, fluid inclusions were examined in gypsum. Numbers printed in bold face denote the dissolution temperatures of halite, which is the last to disappear in inclusions; hence, these temperatures are the homogenization temperatures. In the diagrams, each row of the table corresponds to two points of extreme values (or to a single point, if there is only one value).

**Table 4.** Main parameters of the mineralizing fluid at the Megradzor deposit (data obtained by the study of individual fluid inclusions)

| Fluid parameters | Stages and phases of mineralization | | | | | |
|---|---|---|---|---|---|---|
| | MS | I | II | III | IV | V |
| $T_h$, °C | 465–250 | 360–271 | 328–202 | 272–121 | 175–132 | 165–<50 |
| | (385/37) | (300/40) | (265/51) | (190/306) | (160/20) | (110/27) |
| $P$, bar | 2270–1240 | 2180–470 | 590–180 | 250–130 | – | – |
| | (1790/37) | (1040/67) | (320/50) | (190/23) | | |
| $T_e$, °C | –55/–54 | –41/–33 | –37/–28 | –37/–27 | –55/–4.3 | –35/–30 |
| | (–55/37) | (–36/40) | (–32/51) | (–32/306) | (–47/20) | (–32/27) |
| $C_{NaCl}$, wt % | 55.2/34.7 | 11.8/1.8 | 7.5/1.4 | 18.5/1.4 | 17.7/8.8 | 11.8/2.7 |
| | (44.3/37) | (3.0/40) | (4.2/51) | (6.9/306) | (12.8/20) | (6.7/27) |
| $C_{CO_2}$, mol/kg of $H_2O$ | – | 5.7–2.3 | 5.0/0.9 | Traces | – | – |
| | | (4.1/28) | (2.3/48) | | | |

Note: MS—magnetite skarn phase; I–V stages of the gold-producing hydrothermal phase: I—quartz–hematite–pyrite, II—quartz–chalcopyrite–pyrite, III—gold–galena–sphalerite, IV—gold–silver–telluride, V—postmineralization quartz–carbonate. $T_h$—homogenization temperature, $T_e$—eutectic temperature, $P$—pressure, $C_{NaCl}$—salt concentrations in fluid (equivalent NaCl amounts), $C_{CO_2}$—$CO_2$ concentration in fluid. Numbers in parentheses in numerators are average values; the same in the denominators show the number of inclusions in the sampling.

tion were deposited at notably greater depths than those of "normal" epithermal deposits. At the same time, the correlated pressure and temperature values define a continuous trend of decreasing parameters from the skarn to gold-bearing mineral assemblages. The density of the fluid shows a more complex dependence and decreases with increasing temperature in the early associations (this was, perhaps, caused by a decrease in the concentrations of salts and gases) and increases again at temperatures below 250°C (Fig. 1).

The gold–galena–sphalerite mineralization of stage III was also produced by chloride–magnesian–sodic solutions, but their salinity varied over a broader interval (18.5–1.4 wt % equiv. NaCl) and their temperatures were lower ($T_h$ = 272–121°C). Fluid heterogenization was rarely encountered in these minerals, and we were able to estimate the pressure only for two samples, which yielded much lower values than those of the quartz–chalcopyrite–pyrite association (250–130 bar). Broad variations in the salinity suggest that the fluids responsible for the deposition of mineralization during stages I and II could mix with colder, weakly mineralized vadose waters. In contrast to the fluids of stages I and II, these fluids only rarely display evidence of boiling and carbon dioxide in their gas phase has a low density. The parameters of these solutions are close to those of the mineralizing fluids of epithermal gold–silver–base metal deposits [7, 23].

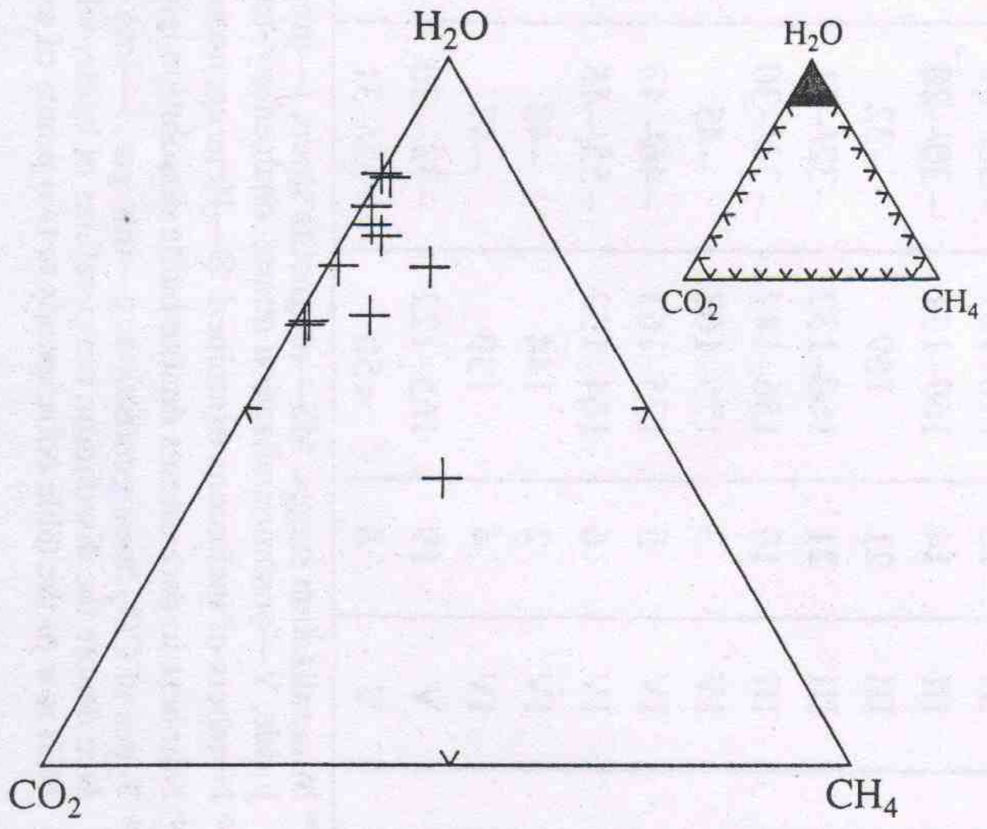


**Fig. 2.** $H_2O$–$CO_2$–$CH_4$ plot showing the results of gas chromatographic analysis of fluid inclusions in minerals from the Megradzor deposit.

The mineralizing solutions preserved as FI in the quartz hosting the gold–silver–telluride mineralization of stage IV differed from the mineralizing fluids of earlier stages. These fluids were characterized by elevated concentrations of salts (their salinity was 17.7–8.8 wt % equiv. NaCl), a relatively low temperature ($T_h$ = 175–132°C), a predominantly chloride–magnesian–calcic or chloride–calcic–sodic ($T_e$ from –55 to –43°C) composition, and an absence of fluid heterogenization (Table 4). They show some similarities with the fluids of epithermal gold–telluride deposits [7].

The bulk composition of the mineralizing solutions was studied by **gas and ion chromatographic techniques**. These results (Table 5) suggest that the ligands of the mineralizing solutions were dominated by the $Cl^-$ ion. However, taking into account the fact that ~70% of our samples had cation sums notably higher

**Table 5.** Bulk concentrations of cations, anions, and volatile components determined in fluid inclusions in quartz from mineralized veins at the Megradzor deposit (ion and gas chromatography determinations)

| Stage | Sample | $H_2O$, μg/g of quartz | Concentration, g/kg of $H_2O$ | | | | | Cations and anion* | | | Volatiles** | | | |
|---|---|---|---|---|---|---|---|---|---|---|---|---|---|---|
| | | | $Na^+$ | $K^+$ | $Cl^-$ | $CO_2$ | $CH_4$ | $Na^+$ | $K^+$ | $Cl^-$ | $H_2O$ | $CO_2$ | $CH_4$ | $H_2S$*** |
| II | 110/87 | 246 | 9.9 | 2.0 | 10.5 | 190 | 3.95 | 0.430 | 0.051 | 0.296 | | 4.3 | 0.2 | – |
| | | | | | | | | 0.99 | 0.20 | 1.05 | 92.48 | 7.18 | 0.34 | |
| | 112/87 | 436 | 7.6 | 0.6 | 8.8 | 146 | 17.0 | 0.330 | 0.015 | 0.248 | | 3.3 | 1.1 | – |
| | | | | | | | | 0.76 | 0.06 | 0.88 | 92.68 | 5.55 | 1.77 | |
| | 119/87 | 378 | 12.3 | 1.5 | 16.4 | 147 | 3.2 | 0.535 | 0.038 | 0.462 | | 3.2 | 0.2 | – |
| | | | | | | | | 1.23 | 0.15 | 1.64 | 94.00 | 5.66 | 0.34 | |
| | 135/87 | 243 | 10.2 | 3.5 | 10.5 | 170 | 58.4 | 0.443 | 0.090 | 0.296 | | 3.9 | 3.6 | 0.04 |
| | | | | | | | | 1.02 | 0.35 | 1.05 | 88.11 | 6.10 | 5.79 | |
| | 139/87 | 414 | – | – | – | 78 | 2.7 | – | – | – | | 1.8 | 0.2 | – |
| | | | | | | | | | | | 96.63 | 3.08 | 0.29 | |
| III | 148/87 | 174 | 13.4 | 5.4 | 27.4 | 87 | 24.1 | 0.583 | 0.138 | 0.772 | | 2.0 | 1.5 | – |
| | | | | | | | | 1.34 | 0.54 | 2.74 | 94.10 | 3.34 | 2.56 | |
| | 79/87 | 533 | 6.8 | 1.2 | 8.7 | 194 | 2.4 | 0.296 | 0.031 | 0.245 | | 4.4 | 0.2 | – |
| | | | | | | | | 0.68 | 0.12 | 0.87 | 92.42 | 7.35 | 0.25 | |
| | 128/87 | 720 | 10.1 | 1.6 | 8.5 | 107 | 8.5 | 0.439 | 0.041 | 0.239 | | 2.4 | 0.5 | – |
| | | | | | | | | 1.01 | 0.16 | 0.85 | 94.94 | 4.16 | 0.90 | |
| IV | 65/87 | 933 | 16.4 | 0.9 | 26.4 | 82 | 0.75 | 0.713 | 0.023 | 0.744 | | 1.9 | 0.05 | – |
| | | | | | | | | 1.64 | 0.090 | 2.64 | 96.67 | 3.25 | 0.08 | |
| | 108/87 | 412 | 11.8 | 1.9 | 8.7 | 103 | 2.7 | 0.513 | 0.049 | 0.695 | | 2.3 | 0.2 | 0.01 |
| | | | | | | | | 1.18 | 0.19 | 2.47 | 95.69 | 4.02 | 0.29 | |
| | 109/87 | 809 | 10.5 | 1.8 | 13.7 | 108 | 5.1 | 0.456 | 0.046 | 0.386 | | 2.4 | 0.3 | 0.01 |
| | | | | | | | | 1.05 | 0.18 | 1.37 | 95.26 | 4.20 | 0.54 | |

Notes: * Upper row—mol/kg of $H_2O$, lower row—wt %; ** upper row—mol/kg of $H_2O$, lower row—mol % (relative); dashes mean not analyzed; *** $H_2S$ was determined potentiometrically.

(by factors of 1.8–1.3) than the anion sums, it can be suggested that the solutions contained hydrocarbonate ions, such as $HCO_3^-$. In the cationic constituent of the solutions, Na usually strongly dominates over K, a fact that was also noted during our cryometric study (Table 3).

Our gas chromatographic results (Table 5) of FI studies confirm cryometric evidence that individual inclusions contain carbon dioxide (Tables 3, 4) and point to the presence of small concentrations of methane. The fairly broad variations in the proportions of $CO_2$ and $CH_4$ (Tables 3–5, Fig. 2) provide evidence for significant fluctuations in the redox conditions during the deposition of mineral assemblages of mineralizing stages. We also identified relatively high concentrations of sulfide sulfur, from $4 \times 10^{-2}$ to $9 \times 10^{-3}$ mol/kg of solution (Table 5), which is consistent with cryometric evidence.

**Isotopic data.** The study of stable isotopes is commonly conducted to clarify the genesis and evolution of a mineralizing solution and to assay the conditions under which ore mineralization was deposited [24–31]. We examined the sulfur isotopic composition of the main ore-forming sulfides and the oxygen isotopic composition of the quartz hosting the gold mineralization.

The isotopic composition of sulfur was determined in pyrite (4 samples), chalcopyrite (1), sphalerite (3), and galena (3), which represent the ore mineralization of the gold-producing hydrothermal stage. The pyrite and chalcopyrite characterize the quartz–chalcopyrite–pyrite (II) stage, whereas the sphalerite and galena belong to the gold–galena–sphalerite (III) stage. Our results are summarized in Table 6. As can be seen from these data, the $\delta^{34}S$ of the sulfides are somewhat heavier than the meteoritic standard and vary within a relatively narrow range: from 3.88 to 5.54‰ for pyrite, from 3.42 to 4.06‰ for sphalerite, and from 1.76 to 2.69‰ for galena. The values obtained for the sulfur isotopic composition of coexisting sphalerite and galena in Samples 79/87 and 148/87 define a fractionation trend ($\delta^{34}S_{Sp} > \delta^{34}S_{Gn}$), which suggests that isotopic equilibrium could be attained between the two minerals. However, the

**Table 6.** Average isotopic composition of sulfur in sulfides and oxygen in quartz from mineralized veins at the Megradzor deposit and calculated sulfur isotopic composition of hydrogen sulfide and oxygen isotopic composition of water

| Sample | Stage | $\delta^{34}S$, ‰ | | | | | | | | $\delta^{18}O$, ‰ | |
|---|---|---|---|---|---|---|---|---|---|---|---|
| | | *Py* | *Cp* | *Sp* | *Gn* | $H_2S_{aq}$(*Py*) | $H_2S_{aq}$(*Cp*) | $H_2S_{aq}$(*Sp*) | $H_2S_{aq}$(*Gn*) | *Q* | $H_2O$ |
| 110/87 | II | 5.54 | | | | 4.16 | | | | 8.50 | 0.27 |
| 112/87 | II | 4.70 | | 3.42 | | 3.32 | | 2.95 | | 9.67 | 1.44 |
| 119/87 | II | | | | | | | | | 7.67 | –0.56 |
| 135/87 | II | | | | | | | | | 8.3 | 0.07 |
| 139/87 | II | 5.69 | | | 1.76 | 4.34 | | | 4.69 | 9.50 | 1.27 |
| 79/87 | III | 3.88 | 3.35 | 4.06 | 2.17 | 2.50 | 3.52 | 3.59 | 5.10 | 7.72 | –4.55 |
| 128/87 | III | | | | | | | | | 6.26 | –6.01 |
| 148/87 | III | | | 3.99 | 2.69 | | | 3.52 | 5.62 | 2.87 | –9.40 |
| 65/87 | IV | | | | | | | | | 13.11 | –1.39 |
| 108/87 | IV | | | | | | | | | 11.09 | –3.41 |
| 109/87 | IV | | | | | | | | | 11.46 | –3.04 |
| Average | | | | | | 3.57 | 3.52 | 3.35 | 5.14 | | |

Note: *Py*—pyrite, *Cp*—chalcopyrite, *Sp*—sphalerite, *Gn*—galena, *Q*—quartz.

values of sulfur-isotopic temperatures, which were calculated by the equation from [19] for sphalerite–galena pairs (473 and 347°C for Samples 79/87 and 148/87, respectively), are notably higher than the homogenization temperatures of FI in the quartz of stage III (270–120°C at an average of 190°C, Tables 3, 4). The possible explanations of the higher values of the sulfur-isotopic geothermometry are as follows: (1) The sphalerite and galena were contaminated with one another—as is usually seen in polished sections, the two minerals compose closely intergrown aggregates. (2) Sulfur-isotopic equilibrium between the sulfides could be readjusted during cooling. (3) Sphalerite and galena belonging to the same mineralization stage were, in fact, deposited sequentially, and, as can be inferred from the relationships between these minerals in polished sections, the galena is younger than the sphalerite. (4) No equilibrium between the sulfides was attained because of the sluggish kinetics of this process. The former three factors (or their combinations) can be regarded as the most probable causes of the overestimates of the sulfur-isotopic temperatures, because, according to [22, 27], the reduced dissolved sulfur of hydrothermal solutions ($H_2S_{aq}$) should be in equilibrium with simple sulfides.

Because the aqueous species $H_2S_{aq}$ dominates among the S-bearing species of mineralizing solutions [22], the bulk S isotopic composition should be close to the S isotopic composition of $H_2S_{aq}$. Assuming that local equilibrium was attained between the deposited sulfides and the mineralizing solution, one can utilize the fractionation factors from [19] and the $\delta^{34}S$ values obtained for the Megradzor ores (Table 6) to assay the $\delta^{34}S$ of $H_2S_{aq}$ in the mineralizing fluid that produced these ores. Table 6 lists the results of these calculations, which were carried out with the use of the average mineralization temperatures for individual stages of the ore-forming process (Table 4). It can be seen that the $\delta^{34}S$ of $H_2S_{aq}$ calculated from the isotopic compositions of pyrite, chalcopyrite, and sphalerite are fairly similar, whereas the analogous values obtained for galena are remarkably higher. These values are generally more isotopically heavy than the $\delta^{34}S$ values of $H_2S_{aq}$ (from 0 to 2‰) thought to be typical of magmatic sulfur [28]. Because the bulk of galena in the Megradzor ores is contained in younger, mostly gold-rich associations of stage III and the earliest associations of stage IV (Table 1), it is hardly probable that the sulfur of $H_2S_{aq}$ in the mineralizing fluid could become significantly isotopically heavier over this brief time period. As has been demonstrated in [1, 6], it was exactly between stages III and IV that the physicochemical parameters and composition of the mineralizing solution were fundamentally changed; this resulted in the transition from sulfide to telluride mineral assemblages and in the massive deposition of gold. Differences between the cationic, anionic, and gas compositions of the mineralizing solutions that produced mineralization during the gold–sulfide (I–III) and gold–silver–sulfide (IV) stages are also apparent from FI data (Fig. 1). Our isotopic results do not provide unambiguous evidence of the sulfur sources, but they fall within the interval of values (from –3 to 9‰) typical of porphyry copper deposits [24]. This means that the sulfur could be mainly of magmatic provenance and was either added by magmatic fluids or leached from sulfides in the country rocks that hosted the mineralization. At the same time, the relatively high $\delta^{34}S$ values of $H_2S_{aq}$ in the mineralizing fluid, particularly its latest portions, may be indicative of the partial mobilization of sulfur from the underlying evaporitic

deposits or connate chloride–calcic–magnesian solutions, whose mixing with early portions of the mineralizing solutions is considered among the deposition factors of the gold–silver–telluride ores [1].

The isotopic composition of *oxygen* was determined in eleven quartz samples (Table 6), which characterize the mineralization of stages II (Samples 110/87, 112/87, 119/87, 135/87, and 139/87), III (Samples (79/87, 128/87, and 148/87), and IV (Samples 65/87, 108/87, and 109/87). All of the $\delta^{18}O$ have positive values, but while these values for quartz of stages II and IV vary within a relatively narrow range (from 7.67 to 9.50‰ and from 11.09 to 13.11‰, respectively), these values for quartz of stage III are characterized by much broader variations (from 2.87 to 7.72‰). This could be caused by the fact that our samples of quartz of stage III represented both the early and late phases of the mineralizing process, which are characterized by significant differences in temperatures and other physicochemical parameters [1]. Moreover, the process of deposition of these mineral assemblages was marked by more significant temperature variations than those from earlier and later stages of the mineralizing process (Table 4). It should also be mentioned that the quartz of the gold–silver–telluride (IV) stage was determined to have remarkably higher $\delta^{18}O$ values than those of the quartz of stages II and III (Table 6).

If the FI were captured at the temperature of equilibrium between the mineralizing fluid and quartz, knowing the $\delta^{18}O$ of the quartz and using the equation for quartz–water equilibrium from [26], it is possible to calculate the oxygen isotopic composition of water in the mineralizing fluid that produced the quartz. The calculated $\delta^{18}O$ for water (at average temperatures for each stage from Table 4) are listed in Table 6. These data demonstrate that the water of the Megradzor mineralizing solutions is notably isotopically lighter than the water of the magmatic fluid (5.5–9.5‰) [28, 29]. At the same time, the water of the fluids of stage II generally exhibited positive $\delta^{18}O$ values (its average $\delta^{18}O_{H_2O}$ is equal to 0.50‰) and its isotopic composition became significantly lighter during the evolution of the mineralizing process (the average $\delta^{18}O$ of $H_2O$ for stages III and IV are, respectively, –6.65‰ and –3.04‰). If these regularities hold for the whole mineralizing process, the water of the solutions that produced mineralization during the early quartz–hematite–pyrite (I) stage could have $\delta^{18}O$ values close to those of magmatic water. In this case, our data on the oxygen isotopic composition are consistent with the data on FI, according to which the cooling trend of the mineralizing fluid during stages I–III could be determined by mixing between relatively hot fluids of predominantly magmatic genesis and cooler meteoric water. The differences between the oxygen isotopic compositions of solutions of stages III and IV could be caused by the fact that, in the latter case, the meteoric water contained isotopically heavier oxygen from formation brines [25].

## EVALUATION OF THE PHYSICOCHEMICAL CONDITIONS OF THE ORIGIN OF GOLD–SULFIDE–TELLURIDE MINERALIZATION

We evaluated the physicochemical conditions under which the Megradzor ores were produced by thermodynamic calculation with the use of databases of thermodynamic constants for equilibria between chloride, hydrosulfide, and hydroxyl (for Au) complexes of metals able to form a stable solid phase. The calculations were conducted for the *P–T* parameters and compositions of mineralizing fluids determined for all stages of the mineralizing process [1].

The calculation results demonstrate that, during mineralizing stage I, metals occurred in the solution predominantly in the form of chloride complexes and the solution was almost saturated with respect to Au but undersaturated with respect to Ag. With the transition to mineralizing stage II (as the temperature decreased by approximately 50°C), the solubility of Au and Ag decreased by, respectively, 1.2 and 0.8 orders of magnitude and this resulted in the relative enrichment of gold the in mineralization produced during this stage. The further cooling of the solution (during stage III) and loss of acid gases brought about a significant increase in pH (by 1.6 units), oversaturation of the solution with respect to base metals, and active deposition of galena and sphalerite. The passage of the bulk of gold from chloride to hydrosulfide types of speciation led to a slight decrease in its solubility. However, as has been demonstrated by the calculations in [1], this decrease was significantly smaller than the simultaneous decrease in the solubilities of silver and base metals. This process accounts for the enrichment of the galena–sphalerite ores in silver. It is realistic to hypothesize that the main causes of the depositions of minerals during mineralizing stages I–III was an increase in pH and a decrease in the temperature, which were caused by the heterogenization of the fluids due to a drastic pressure decrease.

In contrast to the variations in the physicochemical parameters of the mineralizing process during stages I through III, which can be explained by temperature and pressure variations, the onset of the deposition of telluride assemblages during stage IV was characterized by fundamental changes in the state of the solution. Our data on FI testify to an increase in its salinity and changes in the cationic composition. According to the thermodynamic calculations in [1], the $f_{Te_2}/f_{S_2}$ increased by several orders of magnitude. Such fundamental changes cannot be explained by anything but the inflow of solutions of different composition into the system. These newly arriving solutions should have been enriched in tellurium and have a chloride–magnesian–calcic composition. Along with our data on fluid inclusions, the close association of dolomite with the gold–silver–telluride mineralization confirms this concept. Observations indicate that Te-rich minerals were the first to crystallize during this stage; they were fol-

lowed by gold and silver tellurides, with the latter becoming dominant late during this stage. This crystallization succession suggests an increase in the (Au + Ag)/Te and Au/Ag ratios and, according to the calculation data [1], a slight decrease in $f_{Te_2}$ (from $10^{-11}$ to $10^{-13}$) at a practically unchanging $f_{Te_2}/f_{S_2}$ ratio, which was locally buffered by the equilibrium $PbS + 0.5Te_2 = PbTe + 0.5S_2$. According to calculations, the solubility of Ag, which was higher than the Au solubility early during mineralizing stage IV, decreased much more rapidly than the Au solubility with decreasing temperature and this led to Ag enrichment in both the late telluride associations and the telluride mineralization as a whole.

## CONCLUSIONS

Our study of fluid inclusions provided valuable information on the Megradzor deposit. The physical parameters of the mineralizing process were determined to vary within broad limits (Table 4): the temperature varied from 360 to <50°C, the pressure decreased from 2180 to 130 bar, the concentration of salts ranged from 18.5 to 1.4 wt % equiv. NaCl, the $CO_2$ concentration was 5.7–0.9 mol/kg of solution, and the analogous values for $H_2S$ ranged from $4 \times 10^{-2}$ to $1 \times 10^{-2}$ mol/kg of solution. The solution contained Cl (0.77–0.24 mol/kg of solution), Na (0.71–0.30 mol/kg of solution), and K (0.14–0.015 mol/kg of solution). The sulfide associations of the quartz–chalcopyrite–pyrite and gold–galena–sphalerite stages were produced by a single solution, which was originally rich in $CO_2$ and $H_2S$ and evolved concurrently with a gradual and stepwise temperature and pressure decrease and the boiling and devolatilization of the Mg–Na solution. The solution was predominantly magmatic in provenance, as follows from data on the sulfur isotopic composition. Our data on the oxygen isotopic composition are generally consistent with the conclusion that this solution could mix with meteoric water. The telluride mineralization was produced by waters of different types. Using thermodynamic simulations, we traced the behavior of ore-forming components and demonstrated that the deposition of metals was most probably controlled mainly by a pH increase and temperature decrease probably due to mineralizing solution ascent to near-surface levels and mixing with meteoric waters. The deposition of the telluride ores was controlled by the involvement of foreign hydrothermal fluids, which could be related to connate brines.

We have demonstrated that the early hydrothermal mineral assemblages in the area of the Megradzor deposit were formed at relatively high temperatures and pressures from fluids enriched in salts and gases and, perhaps, compositionally close to magmatic fluids. At the same time, the gold-rich mineral assemblages were formed under conditions and from a fluid similar to those of epithermal systems. The similarities between the early and late mineral assemblages testify that deep-seated fluids were involved into the genesis of the Megradzor deposit.

## ACKNOWLEDGMENTS

The authors thank L.P. Nosik and N.I. Savel'eva for conducting the analytical works. This study was supported by the Russian Foundation for Basic Research (project nos. 98-05-64052 and 98-05-64775). We also thank V.B. Naumov for the careful analysis of the form and content of this paper and numerous valuable comments.

## REFERENCES

1. Kovalenker, V.A., Prokof'yev, V.Yu., Levin, K.A., *et al.*, Physicochemical Conditions of Formation of Sulfide–Telluride Mineralization in the Megradzor Ore Field, Armenia, *Geol. Rudn. Mestorozhd.,* 1990, no. 6, pp. 18–35.
2. Amiryan, Sh.O., *Zolotorudnye formatsii Armyanskoi SSR (Geologiya, mineral'nyi sostav, geokhimiya i osobennosti metallogenii)* (Gold Ore Deposits in the Armenian SSR: Geology, Mineral Composition, Geochemistry, and Metallogeny), Erevan: Akad. Nauk Armyan. SSR, 1984.
3. Karapetyan, A.I., *Endogennye rudnye formatsii Pambak-Zangezurskoi metallogenicheskoi zony Malogo Kavkaza* (Endogenous Ore Deposits in the Pambak–Zangezur Metallogenic Zone, Lesser Caucasus), Erevan: Akad. Nauk Armyan. SSR, 1982.
4. Karapetyan, A.I., Boyadzhan, M.T., and Atabekyan, M.Kh., Bonanza Types and Their Locations in a Gold Ore Deposit, *Izv. Akad. Nauk Armyan. SSR, Ser. Nauki o Zemle*, 1984, vol. 37, no. 1, pp. 13–17.
5. Mkhitaryan, D.V. and Arakelyants, S.A., Igneous Veins in the Megradzor Ore Field and Their Role in the Localization of Ore Mineralization, *Izv. Akad. Nauk Armyan. SSR., Ser. Nauki o Zemle*, 1985, vol. 38, no. 3, pp. 30–40.
6. Kovalenker, V.A., Zalibekyan, M.A., Laputina, I.P., *et al.*, Sulfide–Telluride Mineralization in the Mergadzor Ore Field, Armenia, *Geol. Rudn. Mestorozhd.,* 1990, no. 3, pp. 65–81.
7. Kovalenker, V.A., Mineralogical and Geochemical Regularities in the Formation of Epithermal Gold and Silver Deposits, *Doctoral (Geol.–Min.) Dissertation*, Moscow: Inst. Geol. Ore Deposits, Russ. Acad. Sci., 1995.
8. Bodnar, R.J., Revised Equation and Table for Determining the Freezing Point Depression, *Geochim. Cosmochim. Acta*, 1993, vol. 57, pp. 683–684.
9. Bodnar, R.J. and Vityk, M.O., Interpretation of Microthermometric Data for $H_2O$–NaCl Fluid Inclusions, in *Fluid Inclusions in Minerals: Methods and Applications*, Vivo, B. and Frezzotti, M.L., Eds., Pontignano-Sienna, 1994, pp. 117–130.
10. Darling, R.S., An Extended Equation to Calculate NaCl Contents from Final Clathrate Melting Temperatures in $H_2O$–$CO_2$–NaCl Fluid Inclusions: Implications for *P–T*–Isochore Location, *Geochim. Cosmochim. Acta,* 1991, vol. 55, pp. 3869–3871.

11. Klevtsov, P.V. and Lemmlein, G.G., Determination of the Minimum Pressure of Quartz Formation: Quartz Crystals from the Pamirs, *Zap. Vses. Mineral. O–va,* 1959, vol. 88, no. 6, pp. 661–666.
12. Brown, P.E., FLINCOR: A Fluid Inclusion Data Reduction and Exploration Program, *Program and Abstracts of Papers of Second Bienn. Pan-Am. Conf. on Research of Fluid Inclusions*, 1989, p. 14.
13. Brown, P.E. and Lamb, W.M., *P–V–T* Properties of Fluids in the System $H_2O$–$CO_2$–NaCl: New Graphical Presentations and Implications for Fluid Inclusion Studies, *Geochim. Cosmochim. Acta*, 1989, vol. 53, no. 6, pp. 1209–1222.
14. Naumov, V.B., Inclusions in Minerals as Indicators of Pressure and Density of Mineral-forming Media, in *Ispol'zovanie metodov termobarogeokhimii pri poiskakh i izuchenii rudnykh mestorozhdenii* (Studies of Inclusions in Minerals Applied for Prospecting and Exploration of Ore Deposits), Laverov, N.P., Ed., Moscow: Nedra, 1982, pp. 85–94.
15. Bischoff, J.L., Densities of Liquids and Vapors in Boiling NaCl–$H_2O$ Solutions: A *P–V–T–X* Summary from 300°C to 500°C, *Am. J. Sci.*, 1991, vol. 291, April, pp. 309–338.
16. Mironova, O.F., Naumov, V.B., and Salazkin, A.N., Nitrogen in Mineral-forming Fluids: Gas Chromatography of Inclusions in Minerals, *Geokhimiya*, 1992, vol. 37, no. 7, pp. 979–992.
17. Savel'eva, N.I., Prokof'yev, V.Yu., Dolgonosov, A.M., *et al.*, Use of Ion Chromatography for the Analysis of Anion Composition of Fluid Inclusions, *Geokhimiya,* 1988, no. 3, pp. 401–408.
18. Kolpakova, N.N., Determination of Hydrogen Sulfide in Fluid Inclusions in Gangue Minerals, *Geokhimiya,* 1982, no. 2, pp. 271–277.
19. Nosik, L.P., *Izotopnye metody pri izuchenii mineraloobrazovaniya* (Isotopic Methods for Studies of Mineral Deposition), Moscow: Nauka, 1986.
20. Mironova, O.F., Naumov, V.B., and Salazkin, A.N., A Study of Fluid Inclusions Containing Hydrogen Sulfide in Quartz from East Transbaikalia, *Geokhimiya,* 1973, no. 12, pp. 1838–1845.
21. Kozerenko, S.V., Baranova, N.N., Kolpakova, N.N., *et al.*, Antimony, Gold, and Hydrogen Sulfide in Mineral-forming Solutions of Gold Ore Deposits, *Tezisy dokladov konferentsii Termobarometriya i geokhimiya rudoobrazuyushchikh flyuidov* (Abstr. Conf. Thermobarometry and Geochemistry of Ore-forming Fluids), Lvov, 1985, vol. 2, p. 65.
22. Baranova, N.N., Kozerenko, S.V., Grigoryan, S.S., *et al.*, Experimental Data on Gold and Silver Concentrations in Hydrothermal Solutions: Analysis of Fluid Inclusions, *Geokhimiya*, 1980, no. 8, pp. 1146–1157.
23. Bodnar, R.J., Reynolds, T.J., and Kuehn, C.A., Fluid Inclusion Systematic in Epithermal Systems, in *Geology and Geochemistry of Epithermal Systems. Rev. Econ. Geol.*, Berger, B.R. and Bethke, P.M., Eds., 1985, vol. 2, pp. 73–97.
24. Ohmoto, H. and Rye, R.O., Isotopes of Sulfur and Carbon, *Geochemistry of Hydrothermal Ore Deposits*, Barnes, H.L., Ed., New York: Wiley, 1979, 2nd edition, pp. 509–567.
25. Taylor, H.P., Jr., Oxygen and Hydrogen Isotope Relationships in Hydrothermal Ore Deposits, *Geochemistry of Hydrothermal Ore Deposits*, Barnes, H.L., Ed., New York: Wiley, 1979, 2nd edition, pp. 236–277.
26. Matsuhisa, Y., Goldsmith, J.R., and Clayton, R.N., Oxygen Isotopic Fractionation in the System Quartz–Albite–Anorthite–Water, *Geochim. Cosmochim. Acta*, 1979, vol. 43, pp. 1131–1140.
27. Ohmoto, H. and Lasaga, A.C., Kinetics of Reactions between Aqueous Sulfates and Sulfides in Hydrothermal Systems, *Geochim. Cosmochim. Acta*, 1982, vol. 46, pp. 1727–1745.
28. Ohmoto, H., Stable Isotope Geochemistry of Ore Deposits, *Rev. Mineral.*, 1986, vol. 16, pp. 491–559.
29. Sheppard, S.M.F., Characterization and Isotopic Variations in Natural Waters, *Rev. Mineral.*, 1986, vol. 16, pp. 165–183.
30. Zairi, N.M., Glukhov, A.P., and Vasyuta, Yu.V., Isotopic and Geochemical Model of Gold Ore Deposits, *Sov. Geol.*, 1987, no. 6, pp. 101–108.
31. Spasennykh, M.Yu. and Bannikova, L.A., Interpretation of Oxygen and Hydrogen Isotope Variations in Hydrothermal Deposits by Means of Quantitative Dynamic Models, in *Izotopnaya geokhimiya protsessa rudoobrazovaniya* (Isotope Geochemistry of Ore Formation), Moscow: Nauka, 1988, pp. 21–39.
32. Barnes, H.L., Solubility of Ore Minerals, in *Geochemistry of Hydrothermal Ore Deposits*, Barnes, H.L., Ed., New York: Wiley, 1979, 2nd edition, pp. 278–403.